A tale of two rift shoulders and two ice masses:

Le Heron, Daniel P.; Busfield, Marie; Ali, Dilshad; Vandyk, Thomas; Tofaif, Saeed

Published in:
Geological Society Special Publications

DOI:
10.1144/SP475.11

Publication date:
2018

Citation for published version (APA):
Le Heron, D. P., Busfield, M., Ali, D., Vandyk, T., & Tofaif, S. (2018). A tale of two rift shoulders and two ice masses: the Cryogenian glaciated margin of Death Valley, California. *Geological Society Special Publications*, *475*. https://doi.org/10.1144/SP475.11

A tale of two rift shoulders, and two ice masses: the Cryogenian glaciated margin of Death Valley, California.

LE HERON, D.P[1]., BUSFIELD, M.E[2]., ALI, D.O[3]., VANDYK, T[4]., TOFAIF, S[5].

[1]*Department of Geodynamics and Sedimentology, University of Vienna, Althanstrasse 14, A-1090 Vienna, Austria*

[2]*Geography and Earth Sciences, Aberystwyth University, Llandinam Building, Aberystwyth, Ceredigion, SY23 3DB*

[3]*Department of Earth Sciences, Royal Holloway University of London, Egham, Surrey, TW20 0EX*

[4]*Department of Geography, Royal Holloway University of London, Egham, Surrey, TW20 0EX*

[5]*Saudi Aramco P.O. Box 5000. Dhahran 31311, Saudi Arabia*

**Corresponding author's e-mail address: daniel.le-heron@univie.ac.at*

Abstract: The Death Valley area of California, USA, exposes an outstanding record of a Neoproterozoic (Cryogenian) glaciated margin: the Kingston Peak Formation. Despite the quality of exposure, however, the outcrops of glaciogenic strata are fragmentary, forming isolated, laterally offset outcrop belts at the western extremity of the Basin and Range province. Excellent evidence for glacially modulated sedimentation includes (i) ice-rafted dropstones in most ranges, (ii) thick diamictites bearing a variety of exotic (extrabasinal) clasts, (iii) striated clasts, and (iv) local occurrences of glacitectonic deformation structures at the basin margins. In tandem with this, there is a distinct signature of slope collapse processes in many ranges, including (i) up to km-scale olistoliths, (ii) extensional growth fault arrays, (iii) dramatic proximal-distal thickness changes and (iv) basalt occurrences. New sedimentological observations reinforce long-held views of rifting superimposed on glaciation (or vice versa), with both processes contributing to a complex record whereby rift and glacial processes vie for stratigraphic supremacy. We consider that a mechanism of diamictite accumulation in a series of rift-shoulder minibasins produced greatly contrasting successions across the Death Valley area, under the incontrovertible influence of hinterland ice sheets.

The Death Valley area yields world class exposures of Cryogenian strata (Prave, 1999), which record the influence of glaciogenic and rift-related fluxes of sediment into a subaqueous basin (Prave, 1999; Macdonald et al., 2013; Busfield & Le Heron, 2016; Le Heron & Busfield, 2016; Le Heron et al., 2017). During the Cryogenian, two glaciations of potentially global extent have been proposed, the older Sturtian and younger Marinoan (Hoffman & Schrag, 2002), with the record of both glaciations argued to be contained within the lower and upper parts of the Kingston Peak Formation (KPF) in this region (Macdonald et al. 2013). Worldwide, these glaciations have been attributed to cooling under a long-lived and globally synchronous Snowball Earth (see Hoffman et al. 2017 for review). However, arguments against global glaciation have favoured deposition of Cryogenian diamictite-dominated successions as rift-related mass flows subject to a substantially reduced, Alpine-style glacial influence (Eyles & Januszczak, 2004). The Death Valley region offers ideal sections to illustrate the combined influence of glaciogenic sediment flux from marine-terminating ice masses and syn-sedimentary rift activity, where the influence and relative dominance of both sources of sediment can be distinguished. The structural and sedimentological record of the active tectonic regime is variable across the study region, and hence a basin-wide review of the studied sections is provided herein. This review sheds significant light on the palaeogeographic setting of Cryogenian glaciation in this region, offers a blueprint for recognising rift-related sedimentation on a glaciated margin otherwise dominated by glaciogenic sediment flux, and raises questions about the validity of regional chronostratigraphic units where the possibility of diachronous rifting and glaciation remains to be addressed.

The Death Valley region lies toward the west of the Basin and Range province where Cenozoic tectonism, with a significant strike-slip component and localised hyper-extension, has disassembled a once more continuous belt of Neoproterozoic strata (**Fig. 1**A). A range of estimates are available concerning the magnitude of extension which has affected the region since the Mesozoic. Taking into account both Mesozoic compression and Cenozoic extension, Levy and Christie-Blick (1989) estimated an extension factor of about 150%. Dextral strike-slip faults have also offset some of the outcrops, with the Amargosa canyon a notable example (Guest et al., 2003). At a regional scale, palinspastic reconstructions of the eastern part of the area (encompassing the Silurian Hills, Alexander Hills, Kingston Range and Sperry Wash outcrop belts, **Fig. 1** A) show comparatively minor dislocation, with much of the E-W strike-slip motion accommodated by a kink in the Garlock Fault at Owlshead

Mountains (Fridrick and Thompson, 2011). This relatively minor offset of the eastern outcrop belts, alongside their exceptionally high-quality exposure, affords far greater correlation of individual sedimentary sequences, and thus significantly enhances the scope for generating meaningful palaeogeographic reconstructions.

The disparate and disconnected arrangement of Neoproterozoic outcrop belts throughout the Death Valley region has focussed efforts on first order correlation of the KPF (e.g. the stratigraphic framework of Prave, 1999). Macdonald *et al*. (2013) developed the stratigraphic framework of Prave (1999) and proposed a five-fold tectonostratigraphic subdivision of the KPF (TU0-4, Macdonald et al., 2013). Of these, four (TU0 and TU2, 3, 4) were argued to be present in Death Valley. The original stratigraphy of Prave (1999) broadly recognises a basal, non-glacial marine succession (KP1: genetically unrelated to the remainder of the succession), KP2 (a basal diamictite), and KP3 (mass flow deposits, olistostromes). Macdonald *et al*. (2013) considered that KP2 and KP3 were the equivalent of the Sturtian glaciation in Australia, with KP4 its Marinoan counterpart. A well-developed interglacial stratigraphy is not universally present across the Death Valley outcrop belts, but is well expressed in the Panamint Range where various limestones separate KP3 from KP4 diamictites (Miller, 1985; Prave, 1999; Petterson *et al*., 2011). The uppermost diamictites have been argued to represent younger, Marinoan-age deposits (Prave, 1999; Macdonald *et al*., 2013).

Whilst the attempts at stratigraphic subdivision outlined above are valuable, there are certain limitations. Even at comparable stratigraphic levels, lateral lithofacies variations are very pronounced, leading to practical difficulty in applying the five-fold framework routinely across studied sections. The most noteworthy example in this region is the evidence for the younger 'Marinoan' equivalent diamictite (widely referred to as unit KP4; Macdonald et al. 2013). Though recognised as only a locally-developed unit, its presence has been reported throughout the wider Death Valley region, from the westernmost Panamint Range (Miller, 1985; Prave, 1999; Petterson et al., 2011), through the central Saddle Peak Hills within the National Park itself (Creveling et al., 2016), to the Kingston Range and neighbouring outcrops further east (Mrofka & Kennedy, 2011; Macdonald et al., 2013). Yet detailed sedimentological investigation of the latter sections reveals no evidence for a significant break in the stratigraphic succession which would distinguish a younger 'KP4' unit from the predominant 'Sturtian' equivalent strata (units KP2 and KP3). The diamictite facies association present towards the top of the exposed sequence is closely interbedded with

graded sandstones and sandy, matrix-rich conglomerates, genetically continuous with the preceding KP2-3 coarse-clastic strata (Le Heron et al., 2014, 2017; Le Heron and Busfield, 2016). Overall, the diamictite facies represent a proximal component of an overall coarsening-upward sequence. This is interpreted to record progradation of a subaqueous fan during a single protracted glaciation (Le Heron et al., 2017), albeit subject to multiple cycles of ice advance and recession, but lacking robust evidence for a second, considerably younger glaciation.

Death Valley glacial geology at a glance

Given the geographic separation of the various Death Valley outcrop belts for the reasons given above, we provide a synthesis of the stratigraphy and sedimentology of each of the main outcrop belts below. Troxel (1966, 1982) suggested that the KPF exhibited distinct northern and southern facies characteristics, with the two facies groupings recording different source areas. This idea was more fully developed in Wright et al. (1974) who proposed a northern source area (the Nopah uplands) and a southern source area (the Mojave uplands). There have been further attempts to subdivide the outcrop belts into east-west groupings (Mrofka, 2010). Collectively, the KPF records an excellent archive of (i) glacially-influenced sedimentation, and (ii) rift processes, but not all outcrop belts exhibit these characteristics to the same degree. Thus, a systematic evaluation of each outcrop belt is important in order that here the region can be understood as a whole, and a palaeogeographic synthesis can be attempted.

The Sperry Wash section

Located immediately north of the Dumont Dunes along the northern flank of the Amargosa River (see **Fig. 1** for location), the Sperry Wash succession was first logged in 1963 by Bennie Troxel, although the logged section itself was published some time later (Troxel, 1982), where excellent descriptions were provided. Rare striated and facetted clasts were reported in a succession that was estimated to be up to 40% Fe by volume (Troxel, 1982, p. 62). Exactly 50 years later, in March 2013, careful logging of the complete 1 km thick succession to a vertical resolution of 50 cm revealed multiple examples of pebble to boulder-sized lonestones that deflect, warp, or truncate underlying laminae in siltstone and shale

(Busfield and Le Heron, 2016). The complete section, included herein and modified from Busfield and Le Heron (2016) (**Fig. 2** A), illustrates a well-defined coarsening-upward motif over several hundred metres in which interbedded conglomerates, sandstones and mudrocks occur. A thick diamictite interval appears near the top of the unit (**Fig. 2** A). Collation of palaeocurrent data, including ripple foresets, scour marks, and flute casts, point to a predominant SE-directed palaeoflow during deposition with very little deviation from this trend (Busfield and Le Heron, 2016). Large parts of the succession are of outstanding outcrop quality and exhibit 100% exposure over many tens of metres (**Fig. 3** A). Thick, tabular beds of sandstone or conglomerate (**Fig. 3** B) commonly cap multi-metre scale coarsening up intervals; many of these show classic Bouma sequences (**Fig. 3** C). At recurrent intervals, lonestones derived from the Beck Spring Dolomite occur in mudrocks, with clear evidence of lamina deflections beneath them (**Fig. 3** D). Occasionally, dm-thick beds of muddy diamictite occur encased within shales (**Fig. 3** E). In other instances, thick intervals of diamictite toward the top of the succession are interbedded with highly attenuated and strained sandstones (**Fig. 3** F). Other features include dewatering structures (**Fig. 3** G). The recurrent fining-upward trends within individual beds extend to mudrocks, whereby grain size variations can be observed at the cm-scale (**Fig. 3** H).

In spite of the outstanding exposure, and seemingly demonstrative sedimentary structures, the interpretation of the Sperry Wash section is not without controversy. Troxel and his students have traditionally interpreted the boulder-sized lonestones to result from slope foundering, causing large clasts to roll basinwards (Calzia *et al.*, 2000). By contrast, Busfield and Le Heron (2016) interpreted these lonestones as ice-rafted dropstones, an interpretation which is greatly strengthened by comparison to the Kingston Range sections (Le Heron and Busfield, 2016). The interstratified conglomerates, sandstones and mudrocks are collectively interpreted as a spectrum of mass flows ranging from debrites to high and low density turbidites, sourced from a grounded marine ice mass (Busfield and Le Heron, 2016). The overall coarsening upward profile of the succession attests to a progressiveice advance, with the intensely folded and attenuated intervals near the top considered to represent glaciotectonites produced by sub-ice shearing at the grounding line (Busfield and Le Heron, 2016). Considering this evidence, a picture emerges of an ice margin delivering mass flows to the basin. This general picture can be used to guide and develop the interpretations for several other Death Valley sections, as we shall demonstrate below.

The Saddle Peak Hills section

Mapping of the Saddle Peak Hills succession (Macdonald *et al*., 2013) demonstrated that the KPF is cut through by a series of dip-slip faults, making an accurate measured section very difficult indeed. Nevertheless, the Saddle Peak Hills KPF succession comprises a lower c. 300 m thick, intermittently exposed unit that bears great similarity to Sperry Wash, and an upper c. 50 m thick unit that contains large dolostone rafts interpreted to result from gravitational collapse of the Noonday Dolomite cap carbonate facies (Creveling et al., 2016). The basal unit is very ferruginous, and we present a basic sedimentary log herein from the part of it (**Fig. 2** B) which illustrates five key phenomena. These are (i) the occurrence of interbedded conglomerates, sandstones and mudrocks, (ii) the predominance of fining upward cycles at the bed scale, (iii) the development of bedset trends with both coarsening and fining upward motifs over many m of strata, (iv) well-expressed lonestones deflecting underlying laminae and (v) sole marks including grooves and flute casts beneath sandstone beds. Our measured section is faulted into place, with the Beck Spring Dolomite lying directly below it (**Fig. 4** A). Thick diamictite beds, >2 m in thickness, punctuate a succession otherwise dominated by normally-graded beds (**Fig. 4**B). The diamictites show a ferruginous matrix and a dominance of dolostone clasts sourced from the Beck Spring Dolomite (**Fig. 4** C). Lonestone-bearing horizons are sandwiched between normally-graded sandstone beds (**Fig. 4** D). The lonestones are typically cm-sized (**Fig. 4** E, F).

In the Saddle Peak Hills, the diamictites have identical relationships with sandstones and mudrocks as at Sperry Wash, where they are interpreted as debrites interrupting an otherwise turbidite-dominated succession, with a secondary glacial influence to produce dropstones (Busfield and Le Heron, 2016). This suite of features confirms the close similarity between the Saddle Peak Hills and Sperry Wash strata.By comparison to the Sperry Wash area, palaeocurrent data are few, but available measurements (**Fig. 2** B) also support a SE-directed palaeoslope in this area. In both these areas, the stratigraphic position of the strata in a regional context is slightly ambiguous. In the Saddle Peak Hills, Macdonald *et al*. (2013) assigned them to a sub-unit of KP3.

The Kingston Range outcrop belt

The Kingston Range exposes the thickest exposures of the KPF. The deposits increase in thickness from about 500 m thick in the north (Le Heron et al., 2014) to about 2.5 km in the extreme south of the range (Le Heron et al., 2018). The succession was mapped at a regional scale by Calzia et al. (2000) who identified a large number of km-scale megaclasts of carbonate derived from the Crystal Spring Formation and the Beck Spring Dolomite "floating" within the succession. This general trend was borne out by detailed mapping in the central part of the range by Macdonald et al. (2013) who made similar observations. In terms of a general stratigraphic subdivision, Le Heron et al. (2018) proposed that the KPF was divisible into three main stratigraphic units in the southern part of the range, which are: (i) a basal diamictite, (ii) an olistostrome succession, and (iii) a supra-olistostrome succession (Fig. 2 C).

The lithofacies as described by Le Heron et al. (2018) can be summarised as follows. Continuous sections of turbidites characterise the basal part of the supra-olistostrome strata in the Kingston Range (**Fig. 5** A). Sharp-based, normally graded conglomerates appear at intervals (**Fig. 5** B), with abundant lonestones in intercalated shales and sandstones (**Fig. 5** C, D). Toward the top of the supra-olistostrome succession, diamictites appear (**Fig. 5** E), the lower levels of which are intercalated with the graded sandstones. The diamictites include both massive (**Fig. 5** E) and stratified varieties: the latter exhibit excellent dropstone textures (**Fig. 5** F). Clasts have polished to furrowed surfaces (**Fig. 5** G). On closer inspection, some of the polished clast surfaces are striated (**Fig. 5** H).

Overall, the supra-olistostrome interval invites close comparison to Sperry Wash, both in terms of facies (graded sandstone beds punctuated by conglomerates) and stratigraphic motif (complex coarsening-up cycles). These reflect a gravity flow-dominated fan that was fed from a glacial source: the Kingston Range Fan (Le Heron et al., 2018). Given the context, and the exquisite deformation structures beneath many of the lonestones, an ice-rafting mechanism seems most likely.

The regional palaeogeographic perspective of Le Heron and Busfield (2016) proposes a northern (Nopah) ice sheet that flowed to the SE (**Fig. 1** B). Six lines of evidence underpin the interpretation of a SE-dipping palaeoslope in the Kingston Range. These are: (i) dramatic thickness variations from Beck Spring Canyon to the southernmost Kingston Range, from c. 350 m to > 5 km; (ii) NW-SE striking faults that show clear evidence of stratal thickening on downthrown blocks to the SE (Walker *et al*., 1986; Le Heron, 2015); (iii) sedimentological

evidence for flow evolution from debrites to low-density turbidites to the SE across the range, (iv) the existence of an olistostrome complex apparently derived from the NW-SE striking fault array that is not present to the NW; (v) dominant SE palaeocurrents recorded throughout the range, particularly in the low density turbidites exposed in the south of the range; (vi), at a local scale, evidence for bed thinning and stratal pinchout in a southeastward direction over several hundred metres. Thus, integrating these lines of evidence, we view the Kingston Range belt simply as a continuation of the Sperry Wash / Saddle Peak Hills slope. This slope drained the Nopah Highlands of Wright *et al*. (1974).

The Silurian Hills outcrop belt

The existence of diamictites equivalent to the KPF in the Silurian Hills was demonstrated during mapping campaigns almost 60 years ago (Kupfer, 1960). Since that time, until very recently the only detailed study in this outcrop belt was contained in the MS thesis of Basse (1978). A 1.4 km thick sedimentary log for this belt (**Fig. 2** D) underscores the predominance of thick diamictite deposits together with lonestone-bearing, heterolithic deposits. Le Heron et al. (2017) recognised two distinct types of diamictite: (i) a boulder-bearing diamictite and (ii) a megaclast-bearing diamictite, which are repeatedly stacked throughout the 1.4 km thick succession (Fig. 7A).Clasts in the boulder-bearing diamictites predominantly comprise quartzite, felsic gneiss and schist, with some metabasite (schist grade) (**Fig. 7** B). They are punctuated at intervals by heterolithic deposits characterised by repeated, bed-scale fining upward sequences (**Fig. 7** C). Dropstones occur in multiple horizons (**Fig. 7** D) and are typically composed of crystalline basement material (i.e. gneiss, schist, and granite).

Given that the clasts are of the same composition to the dropstones, the boulder-bearing diamictites were proposed to be derived from a glacial source. The megaclast diamictites, by contrast, were argued to be derived from slope failure and syn-sedimentary fault activity, essentially recording the collapse of a carbonate platform sequence that mantled the crystalline basement. The glacial “conveyor belt” supplied far travelled clasts both to boulder-bearing diamictites and as dropstones in heterolithic deposits, whilst megaclasts were largely supplied through foundering of the sedimentary succession that underlies the KPF. In sum, the sedimentological observations above are consistent with a subaqueous fan complex as first proposed by Basse (1978), with the newly recognised glacial influence (Le Heron et al., 2017) superimposed. This, together with the occurrence of

lonestones throughout the more heterolithic parts of the succession (**Fig 7** D) underscores a broadly common depositional environment to that identified further north in Sperry Wash. The key difference, as noted by Troxel (1966, 1982), is the *composition* of the lonestones and the predominance of basement lithologies in the boulder-bearing diamictite. The reason for this is the derivation of these from a southern source (the Mojave uplands: Wright et al., 1974).

The Southern Salt Spring Hills

This region was last examined in the mid-1960s, when it was mapped by Troxel (1967). In 2016, two of us (Le Heron and Vandyk) re-examined Troxel's units pЄka-pЄke: the mapping units which we interpret to belong to the KPF. We present a sketch log for part of this range (**Fig. 8**). All rocks have been contact metamorphosed to varying degrees as a result of the emplacement of a quartz diorite which underlies the range (Troxel, 1967). The base of the KPF is not exposed, and the succession commences with trough cross-bedded quartzites. Intervals of dolostone also occur low down in the succession. Unlike the other ranges, an accurate sedimentary log is virtually impossible owing to metamorphism and / or tectonic activity which have imparted a highly rubbly appearance to the outcrop (**Fig. 9** A), meaning that even where well bedded strata are recognised, it is difficult to measure true thicknesses accurately. Massive, dark-coloured, ferruginous diamictites (**Fig. 9** B) dominate the lower portion of the succession (**Fig. 9**), which are rich in gneiss, schist, quartzite and granite clasts varying from pebble to boulder size. The diamictite is punctuated by rare m-thick intervals of delicately laminated strata which contain abundant lonestones (**Fig. 9** C). The middle part of the KPF is dominated by similar ferruginous laminites (**Fig. 9** D): these contain delicate flame structures, soft-sediment folds, and are interrupted by granite-rich pebble trains and rare m-size boulders. The upper part of the KPF is very intermittently exposed but is characterised by stacked, normally-graded beds of arkosic granular conglomerate, sandstone and siltstone. Some of the bedsets are, in turn, arranged into decametre-scale coarsening upward intervals. The composite thickness of the KPF was estimated at 3600 ft (ca. 1100 m) by Troxel (1967): however, given the very poor bedding continuity, and difficulty in measuring true thicknesses in this range, it is possible that this is an over-estimation.

The nature of the exposure means that this section must be interpreted with great caution. Nevertheless, phenomena in common with the Silurian Hills succession further to the east

include the dark-colour of the diamictites, which contrasts with all other sections described above, and the presence of lonestones in heterolithic strata: the deflected laminae beneath the clasts allow us to interpret them as dropstones. Unfortunately, in all other respects, the fragmentary data (no palaeocurrent information, low resolution logs, discontinuous exposure) generally preclude us from integrating this substantial outcrop into a regional model.

The Panamint Range

Although at the time of writing (2017), none of the authors have worked on the Panamint Range in detail, we summarise the detailed work of others for completeness as it contains the third thickest section of the KPF in the Death Valley area (after the Kingston Range and the Silurian Hills). Much of the region was mapped by Labotka *et al*., (1980), and the KPF was differentiated into various members and sub-members by these workers. In ascending stratigraphic order, these units are the Limekiln Spring, Surprise and Sourdough Limestone members, and the overlying Middle Park and Wildrose sub-members. E-W oriented canyons dissect the Kingston Peak stratigraphy, and these allowed Miller (1985) to describe the strata throughout much of the range: the basis of her depositional model. Essentially, regional correlation has proposed that the Limekiln Spring Formation is equivalent to the unit KP2 diamictite in the eastern Death Valley area, the Surprise Member through Middle Park Sub-Member correlates to KP3, whereas the Wildrose Diamictite matches with KP4 in the east (Macdonald *et al*., 2013).

Miller (1983, 1985) established a depositional model in which a northward dipping palaeoslope was interpreted during deposition of the Limekiln Spring member. Onlap against crystalline basement to the south of the Goler Wash area was noted earlier (Labotka *et al*., 1980), with normal faults downstepping to the north. Large blocks of material were described in diamictites of the latter canyon, and cited as evidence for slope collapse and olistostrome generation during regional rifting (Prave, 1999). The Goler Wash sections also exhibit spectacular diamictites that bear close comparison to the boulder-bearing diamictites described by Le Heron et al. (2017) in the Silurian Hills (**Fig. 10** A). They attain several hundred metres in thickness. Basalts with a MORB-type composition in the Surprise Member (Labotka *et al*., 1980) imply that rift-related tectonic processes played a key role in the generation of the regional slope in this area (Petterson *et al*., 2011). Some possible, albeit faint, outlines of pillow lava geometries can be observed in Pleasant Canyon (**Fig. 10** B).

Overall, the work of Miller (1985) is made all the more remarkable owing to the degree of deformation and metamorphism in the southern and central part of the range. However, given the recent re-interpretation of igneous intrusions as olistoliths in the Silurian Hills KPF (Vandyk et al., 2018), along with the very limited geochemical dataset available for these metamorphosed Panamint basalts (Hammond, 1983), it is suggested that these sections now urgently need re-evaluation to determine whether the metabasites in the Panamints are actually lavas rather than remobilised slabs of older igneous rocks. Miller (1985) deduced that northward thickening from 40 m to > 1000 m in this member, in concert with downtract facies changes from diamictite to greywacke and pelites, lent support to the interpretation of a north-sloping shelf. She interpreted the diamictite as a lodgement till or glaciomarine deposit, and the greywackes as turbidites.

A tale of two rift shoulders, and two ice masses

There are multiple lines of evidence that the Death Valley area was a rifted glaciated margin during deposition of the KPF. These lines of evidence are outlined below, and then expanded upon in detail in the following section. The Death Valley area serves as an exemplar for the delivery of material to a rifted basin from two rift shoulders via two different ice masses, producing markedly contrasting stratigraphy in the various outcrop belts.

The rift margins

Troxel (1966, 1982) made the powerful observation that a northern facies and a southern facies could be recognised from clast content. In the northern facies, carbonate clasts derived from underlying units such as the Crystal Spring and Beck Spring formations are predominant, whereas in the southern facies, crystalline basement lithotypes (notably gneiss, schist, metabasite, granitoid and quartzite) are much more common (Troxel 1966, 1982). Different source areas are hence implied, and in palaeogeographic terms, two upland areas were posited as source areas for the clasts: a Mojave Upland which drained to the north, and a Nopah Upland which drained in approximately the opposite direction toward the south (Wright *et al*., 1974). The existence of opposing palaeoslopes was strong circumstantial evidence for the presence of a failed rift running approximately E-W and occupied by the present day Amargosa canyon: the Amargosa aulacogen (Wright *et al*., 1974). Palaeocurrent

analysis supports the concept of northern and southern source areas (e.g. Le Heron and Busfield, 2016). These source areas reflect the delivery of material from two upland regions (to the present day north and to the present day south). As will be shown below, these upland regions correspond to two rift shoulders.

Whilst the concept of an aulacogen in the Amargosa area has subsequently fallen out of favour (see Mahon *et al*., 2014), strong evidence for rifting during Kingston Peak time remains. Critical to this interpretation are intercalated MORB-type pillow lavas (Hammond, 1983) in the Panamint Range on the western Death Valley flank (Labotka *et al*., 1980), within the so-called Surprise Member (Miller, 1985). Furthermore, en echelon growth faults in the Kingston Range are interpreted as the signature of a rift margin (Walker *et al*., 1986). This extensional fault array is known to have been the source area for megaclasts (Terry and Goff, 2014) within the KPF (Le Heron, 2015). The major lateral thickness variations across the Death Valley area are also compatible with rift-generated accommodation space (Prave, 1999).

Converging ice masses

Although northern and southern source areas can be distinguished by clast content (Troxel, 1966), in practice the effects of Cenozoic strike-slip tectonics has produced a major challenge for any meaningful palaeo-ice sheet reconstruction. The most continuous outcrop belt lies in the Panamint Range immediately west of Death Valley (**Fig. 1**), where metasedimentary rocks extend for up to 100 km from N-S, locally reaching amphibolite facies. The presence of two ice centres in the Panamint Range seems likely, in the Goler Wash area to the south and on the so-called World Beater dome further north (Miller, 1985; Prave, 1999). Yet it remains highly uncertain how, if at all, these ice masses connected with those in the eastern Death Valley area, and substantial additional work is required to resolve this issue. Outcrops of much lower quality occur elsewhere, including the Black Mountains at the eastern flank of Death Valley. In terms of a regional picture, on the basis of detrital zircon analysis and provenance studies, the Death Valley area could be posited to be a regional basin during KPF time, thus receiving sediment from all sides and not just the north and south (Mahon et al., 2014b).

In spite of the Cenozoic tectonic overprint noted above, Le Heron and Busfield (2016) were able to propose a palaeogeographic reconstruction and ice sheet reconstruction for a small area of eastern Death Valley, encompassing the Kingston Range, Sperry Wash and Silurian Hills areas *(***Fig. 1** B*).* A grounding zone was recognised in the Sperry Wash area on account of a thick diamictite with delicately intercalated soft-sediment deformation interpreted as glaciotectonic structures (Busfield and Le Heron, 2016), and a fjordal setting was suggested. This area was viewed as proximal to much of the Kingston Range, with identical (SE-directed) palaeocurrents measured from medial and distal turbidite sandstones throughout the succession (Le Heron et al., 2018). All of these areas are dominated by carbonate clasts and detritus. By contrast, the completely different character of the Silurian Hills succession, being dominated by crystalline basement detritus and exhibiting N-directed palaeocurrents (Basse, 1980) underscores the idea of provenance from a separate ice mass. The glaciogenic affinity of the diamictites in the Silurian Hills area has subsequently been demonstrated (Le Heron et al., 2017).

The case for diachronous rifting and diachronous glaciation

The recent discovery of dropstones in both the Silurian Hills (Le Heron et al., 2017) and in the Salt Spring Hills, the latter presented for the first time herein, is very significant because it provides affirmation that the KPF is indeed present at the expected stratigraphic levels. For example, given the presence of cobble-bearing diamictites in strata beneath the KPF in the Silurian Hills (interpreted as fluvial deposits: Basse, 1978), miscorrelation is clearly possible. Thus, the presence of dropstones set the scene for testing models that promote the interpretation of regionally extensive stratigraphic units of the KPF.

In the Kingston Range, Walker *et al*. (1986) interpreted evidence for syn-depositional extension from within the KPF near Horsethief Springs. In map view (**Fig. 11** A, B), evidence for growth strata includes the thickening of units onto hanging-wall blocks in the north of that range. From a global perspective, Eyles and Januszczak (2004) posited that Cryogenian glaciation occurred diachronously, with ice sheets selectively populating the rift shoulders of an unzipping Rodinia supercontinent. Their model cautioned that lithostratigraphic correlation of Cryogenian diamictites may not take into account the expected diachroneity, a point also made in age compilations for Neoproterozoic diamictites by Allen and Etienne (2008) and Spence et al. (2016). At the scale of Death Valley, it has

been proposed that the diamictite-bearing units can be correlated between many of the constituent outcrop belts (e.g. between the Kingston Range, the Saddle Peak Hills, the Silurian Hills and the Panamints) (Prave, 1999), with later work advocating that they are essentially chronostratigraphic markers that form the basis of tectonostratigraphic units across the north American Cordillera (Macdonald *et al*., 2013). Noting this, Le Heron *et al*. (2017) questioned the validity of this claim because at least four diamictite intervals of glacial origin in the Silurian Hills (**Fig. 2** D, **Fig. 11** C), representing at least four localised pulses of glaciation, were proposed in that paper. These glacial diamictites are intercalated with at least four olistostrome intervals which contain obvious 30-100 m wide carbonate megaclasts (**Fig. 11** D, E). This stratigraphic record differs substantially from that in the southern Kingston Range, where a lower and an upper diamictite are recognised (Le Heron *et al*., 2018), sandwiching a single olistostrome. Even the most basic comparison between the logs (**Fig. 2** C, D) identifies major differences in stratigraphy in these study areas, which may result from diachroneity of glacial sediment input, in conjunction with asynchronous activation of basin-bounded faults which might be expected in a rift system. Here, we propose that the different stratigraphy in the Silurian Hills and in the Kingston Range can simply be explained by separate ice masses feeding separate minibasins in an evolving rift system. This model acknowledges both the strong glacial control on sedimentation, and the rifting context, explaining why diamictites cannot be correlated from one outcrop belt to another. Neighbouring ranges preserve different stratigraphy because they represent different minibasins in the rift system, explaining not only the dramatic thickness variations from range to range, but also the number of olistostromes (if present) in each range.

Vandyk *et al*. (2018) examined metabasite igneous bodies in the Silurian Hills which were previously mapped and interpreted as sills (Kupfer, 1960; Basse, 1978). In summary, metabasite bodies in both the Kingston Range and in the Silurian Hills were found to yield U-Pb apatite ages of approximately 1.1 Ga, which are remarkably close in age to the 1.05 Ga diabase intrusions in the underlying Crystal Spring Formation (Heaman and Grotzinger, 1992). Based on geochemical arguments, in conjunction with evidence for disaggregated blocks of metabasite within the diamictites, a revised interpretation of elongate, bedding parallel metabasite olistoliths was proposed. These new interpretations challenged the conventional wisdom on syn-glacial magmatism in the eastern Death Valley area. Given this, they raise regional questions about the degree of magma production during glaciation, and indeed whether long described pillow basalts in diamictites in the Surprise Member in the

448 Panamint Range (west of Death Valley) (Labotka *et al*., 1980; Miller, 1985) were emplaced
449 onto a glaciated sea floor or whether these, too, are olistoliths of older basaltic material.
450 Stratigraphic models through the succession in the Panamint Range (**Fig. 11** F) certainly
451 suggest that this hypothesis demands further investigation.

452 In spite of the complexities outlined above, two patterns emerge: (i), there is excellent
453 evidence for glacial processes recorded in almost all of the outcrop belts of the KPF and (ii),
454 facies variations, and stratigraphic stacking patterns, are sufficiently dramatic to question
455 assertions that tectonostratigraphic units can be confidently identified. Regarding the first
456 point, new data from the Salt Spring Hills allow excellent dropstones to be recognised for the
457 first time. With regard to the second issue, tentative palaeogeographic maps (**Fig. 1**) precis
458 this problem: it is unsurprising that convergent ice masses, from opposite source areas,
459 produce different stacking patterns, and it is unsurprising that at the local scale these ice
460 masses may have behaved diachronously. It should be noted that the complete lack of
461 *absolute* geochronological control on the KPF *does not* mean that the idea of broadly
462 synchronous ice masses feeding the basin(s) should be dismissed immediately. Within the
463 framework of a synchronous glaciation, it is possible that neighbouring glaciers advance and
464 retreat slightly out of phase. However, observation of modern valley glaciers in Nepal, for
465 example, demonstrates synchronous patterns of retreat in response to climate forcing
466 (Bajracharya and Mool, 2009). In combination, the issues discussed above make attempts to
467 assign tectonostratigraphic significance to the diamictite strata premature at present,
468 especially considering that the only absolute age dates from the strata appear to derive from
469 olistoliths (Vandyk *et al*., 2018), although it should be acknowledged that excellent detrital
470 zircon data are available (Mahon *et al*., 2014a, b). Thus, the rocks await considerable and
471 continued work to gain a fuller picture of the Neoproterozoic rifted glaciated margin of Death
472 Valley, California.

473

474 **Conclusions**

475 • Evidence for glaciation in the KPF is excellent throughout the eastern Death Valley
476 area, with the presence of unequivocal dropstones leaving no doubt that the KPF can
477 be correlated as a unit. Their recent discovery in locations such as the Salt Spring
478 Hills and the Silurian Hills (Le Heron et al., 2017) considerably extends the “proven”
479 extent of the glaciogenic facies;

- In general terms, a setting of subaqueous, glaciogenic debris flows, feeding glaciomarine turbidites is envisaged across the region, with dropstones advected through ice rafting. Set against a probable fjordal setting, a picture of two ice sheets flowing from north to south (the Nopah ice sheet) and from south to north (the Mojave ice sheet) emerges, and sets the context for Cryogenian glaciation in this area. The relationship of ice masses between the Panamint Range and the eastern Death Valley outcrops remains conjectural and requires substantial further work;

- Basic comparison of the thickest sections of the KPF in the type area (Kingston Range) and in the Silurian Hills underscores how difficult it is to correlate this formation between neighbouring ranges. With this in mind, and in the absence of any absolute age constraints for the KPF, arguments for regional chronostratigraphic units are premature. It is equally likely that the individual diamictites were deposited diachronously across the different ranges;

- In most ranges, the sedimentary record demonstrates that that glacial input and non-glacial processes (slope failure) vied for stratigraphic supremacy. Evidence for syn-sedimentary faulting during deposition of the KPF is recognised in three outcrop belts, namely the Kingston Range, the Silurian Hills, and in the Panamint Range, upholding the long-held view of rifting superimposed on glaciation, or vice-versa. We propose a model for the regional accumulation of the KPF whereby glacial and non-glacial (slope) diamictites accumulated together in rift-shoulder minibasins, producing locally contrasting stratigraphy. This model stands in stark contrast to previous work that viewed the individual diamictites as regional chronostratigraphic units.

Acknowledgments

We are very grateful to the Geological Society of London for multiple grants from 2012 to 2016 that has supported five field seasons in the Death Valley area and multiple research projects of our group. We are thankful to the two anonymous reviewers who provided some excellent suggestions for improvement. We also acknowledge excellent discussions about the KPF and Death Valley geology in general from Professor Tony Prave, Professor Darrel Cowan, Professor Carol Dehler. We could not conclude without acknowledging Cynthia Kienetz for her outstanding hospitality, friendship and accommodation in Tecopa.

References

ALLEN, P.A. & ETIENNE, J.L. 2008. Sedimentary challenge to snowball Earth. *Nature Geoscience*, **1**, 817–825.

BAJRACHARYA, S.R. & MOOL, P. 2009. Glaciers, glacial lakes and glacial lake outburst floods in the Mount Everest region, Nepal. *Annals of Glaciology* **50**, 81-86.

BASSE, R.A. 1978. Stratigraphy, Sedimentology and Depositional Setting of the Late Precambrian Pahrump Group, Silurian Hills, California. MS Thesis, Stanford University, 86p.

BUSFIELD, M.E. & LE HERON, D.P. 2016. A Neoproterozoic ice advance sequence, Sperry Wash, California. *Sedimentology*, 63, 307–330.

BUSFIELD, M.E. & LE HERON, D.P. 2018. Snowball Earth under the microscope. *Journal of Sedimentary Research*.

CALZIA, J.P., TROXEL, B.W., WRIGHT, L.A., BURCHFIEL, B.C., DAVIS, G.R., MCMACKIN, M.R. 2000. Geologic map of the Kingston Range, southern Death Valley, California. *USGS Open File Report 2000-412*.

CREVELING, J.R., BERGMANN, K.D. & GROTZINGER, J.P., 2016. Cap carbonate platform facies model, Noonday Formation, SE California. *Geol. Soc. Am. Bull*. **128** (7–8), 1249–1269.

EYLES, N., & JANUSZCZAK, N. 2004. 'Zipper-rift': A tectonic model for Neoproterozoic glaciations during the breakup of Rodinia after 750 Ma. *Earth-Science Reviews*, **65**, 1-73.

FRIDRICK, C.J. & THOMPSON, R.A. 2011. Cenozoic Tectonic Reorganizations of the Death Valley Region, Southeast California and Southwest Nevada. *U.S. Geological Survey Professional Paper 1783, 36 p. and 1 plate*.

GUEST, B., PAVLIS, T.L., GOLDING, H. & SERPA, L. 2003. Chasing the Garlock: A study of tectonic response to vertical axis rotation. *Geology*, **31**, 553-556.

HAMMOND, J.L.G., 1983. Late Precambrian diabase intrusions in the southern Death Valley region, California: Their petrology, geochemistry, and tectonic significance. PhD thesis, University of Southern California.

HEAMAN, L.M. & GROTZINGER, J.P. 1992. 1.08 Ga diabase sills in the Pahrump Group, California: implications for development of the Cordilleran miogeocline. *Geology*, **20**, 637–640.

HOFFMAN, P.F. & SCHRAG, D.P. 2002. The snowball Earth hypothesis: testing the limits of global change. *Terra Nova*, **14**, 129-155.

HOFFMAN, P.F. ABBOT, D.S., ASHKENAZY, Y., BENN, D.I., BROCKS, J.J., COHEN, P.A.,COX, G.M., CREVELING, J.R., DONNADIEU, Y.,ERWIN, D.H., FAIRCHILD, I.J., FERREIRA, D., GOODMAN, J.C., HALVERSON, G.P., JANSEN, M.J., LE HIR, G., LOVE, G.D., MACDONALD, F.A., MALOOF, A.C., PARTIN, C.A., RAMSTEIN, G., ROSE, B.E.J., ROSE, C.V., SADLER, P.M., TZIPERMAN, E., VOIGT, A., & WARREN, S.G. 2017. Snowball Earth climate dynamics and Cryogenian geology-geobiology. Science Advances 3, E1600983. DOI: 10.1126/SCIADV.1600983

KUPFER, D.H. 1960. Thrust faulting and chaos structure, Silurian Hills, San Bernadino County, California. *GSA Bulletin*, **71**, 181-214.

LABOTKA, T.C., ALBEE, A.L., LANPHERE, M.A. & MCDOWELL, S.D. 1980. Stratigraphy, structure and metamorphism in the central Panamint Mountains (Telescope Peak quadrangle), Death Valley area, California, *Geological Society of America Bulletin*, **91**, 843–933.

LE HERON, D.P. 2015. The significance of ice-rafted debris in Sturtian glacial successions. *Sedimentary Geology*, **322**, 19-33.

LE HERON, D.P. & BUSFIELD, M.E. 2016. Pulsed iceberg delivery driven by Sturtian ice sheet dynamics: An example from Death Valley, California. *Sedimentology*, **63**, 331-349.

LE HERON, D.P., BUSFIELD, M.E. & PRAVE, A.R. 2014. Neoproterozoic ice sheets and olistoliths: multiple glacial cycles in the Kingston Peak Formation, California. *Journal of the Geological Society, London*, **171**, 525–538.

LE HERON, D.P., TOFAIF, S., VANDYK, T., ALI, D.O. 2017. A diamictite dichotomy: Glacial conveyor belts and olistostromes in the Neoproterozoic of Death Valley, California, USA. *Geology*, **45**, 31-34.

LE HERON, D.P., BUSFIELD, M.E., ALI, D.O., AL TOFAIF, S. & VANDYK, T.M. 2018. The Cryogenian record in the southern Kingston Range, California: The thickest Death Valley succession in the hunt for a GSSP. *Precambrian Research*, http://dx.doi.org/10.1016/j.precamres.2017.07.017

LEVY, M. & CHRISTIE-BLICK, N. 1989. Pre-Mesozoic Palinspastic Reconstruction of the Eastern Great Basin (Western United States). *Science*, **245**, 1454-1462.

MACDONALD, F.A., PRAVE, A.R., PETTERSON, R., SMITH, E.F., PRUSS, S.B., OATES, K., TROTZUK, D. & FALLICK, A.E. 2013. The Laurentian record of Neoproterozoic glaciation, tectonism, and eukaryotic evolution in Death Valley, California. *Geological Society of America Bulletin*, **125**, 1203–1223.

MAHON, R.C., DEHLER, C.M., LINK, P.K., KARLSTROM, K.E. & GEHRELS, G.E. 2014a. Geochronologic and stratigraphic constraints on the Mesoproterozoic and Neoproterozoic Pahrump Group, Death Valley, California: A record of the assembly, stability, and breakup of Rodinia. *Geological Society of America Bulletin*, **126**, 652-664.

584 MAHON, R.C., DEHLER, C.M., LINK, P.K., KARLSTROM, K.E. & GEHRELS, G.E. 2014b. detrital
585 zircon provenance and paleogeography of the Pahrump Group and overlying strata, Death
586 Valley, California. *Precambrian Research*, **251**, 102-117.

587 MILLER, J.M.G. 1983. Stratigraphy and sedimentology of the upper Proterozoic Kingston
588 Peak Formation, Panamint Range, eastern California. PhD Thesis, Santa Barbara,
589 California, University of California, 335 pp.

590 MILLER, J.M.G. 1985. Glacial and syntectonic sedimentation: The upper Proterozoic
591 Kingston Peak Formation, southern Panamint Range, eastern California. *Geological*
592 *Society of America Bulletin*, **96,** 1537-1553.

593 MROFKA, D. 2010. Competing models for the timing of Cryogenian Glaciation: Evidence
594 from the Kingston Peak Formation, southeastern California. PhD dissertation, University
595 of California, Riverside.

596 MROFKA, D. & KENNEDY, M. 2011. The Kingston Peak Formation in the eastern Death
597 Valley region. *In*: ARNAUD, E., HALVERSON, G.P. & SHIELDS-ZHOU, G. (eds) *The*
598 *Geological Record of Neoproterozoic Glaciations*). Geological Society, London,
599 Memoirs, **36**, 449-458.

600 PETTERSON, R., PRAVE, A.R. & WERNICKE, B.P. 2011. Glaciogenic and related strata of the
601 Neoproterozoic Kingston Peak Formation in the Panamint Range, Death Valley region,
602 California. In: *The Geological Record of Neoproterozoic Glaciations* (Eds E. Arnaud, G.P.
603 Halverson and G. Shields-Zhou). Geological Society, London, Memoirs, **36**, 449-458.

604 PRAVE, A.R. 1999. Two diamictites, two cap carbonates, two $\delta^{13}C$ excursions, two rifts: the
605 Neoproterozoic Kingston Peak Formation, Death Valley, California. *Geology*, **27**, 339-
606 324.

607 SPENCE, G.H., LE HERON, D.P., & FAIRCHILD, I.J. 2016, Sedimentological perspectives on
608 climatic, atmospheric and environmental change in the Neoproterozoic Era.
609 *Sedimentology*, **63**, 253–306.

610 TERRY, J.P. & GOFF, J. 2014. Megaclasts: proposed revised nomenclature at the coarse end of
611 the Udden-Wentworth grain-size scale for sedimentary particles. *Journal of Sedimentary*
612 *Research*, **84**, 192-197.

613 TROXEL, B.W. 1966. Sedimentary Features of the Later Precambrian Kingston Peak
614 Formation, Death Valley. *Geological Society of America Special Paper* **101**, California
615 341 p.

616 TROXEL, B.W. 1967. Sedimentary rocks of the Late Precambrian and Cambrian age in the
617 southern Salt Spring Hills, southeastern Death Valley, California. *California Division of*
618 *Mines and Geology*, **SR92**, 33-41.

619 TROXEL, B.W. 1982, Description of the uppermost part of the Kingston Peak Formation,
620 Amargosa Rim Canyon, Death Valley region, California. *In:* COOPER, J.D., TROXEL, B.W.,

& WRIGHT, L.A. (eds), Geology of Selected Areas in the San Bernardino Mountains, Western Mojave Desert, and Southern Great Basin, California: Volume and Guidebook for Field Trip No. 9, 78th Anniversary Meeting of Cordilleran Section, Geological Society of America. Shoshone, California, Death Valley Publishing Company, 61–70.

VANDYK, T.M., LE HERON, D.P., CHEW, D.M., AMATO, J.M., THIRLWALL, M., DEHLER, HENNIG, J., CASTONGUAY, S.R., KNOTT, T., TOFAIF, S., ALI, D.O., MANNING, BUSFIELD, M.E., DOEPKE, D. & GRASSINEAU, N. 2018. Precambrian olistoliths masquerading as sills from Death Valley, California. *Journal of the Geological Society, London*. https://doi.org/10.1144/jgs2017-002

WALKER, J.D., KLEPACKI, D.W., & BURCHFIEL, B.C. 1986. Late Precambrian tectonism in the Kingston Range, southern California: *Geology*, **14**, 15–18.

WRIGHT, L.A., TROXEL, B.W., WILLIAMS, E.G., ROBERTS, M.T. & DIEHL, P.E. 1974. Precambrian sedimentary environments of the Death Valley region, eastern California and Nevada. In: *Geological Society of America, Guidebook: Death Valley region, California and Nevada* [prepared for the 70th Annual Meeting of Cordilleran Section, Geological Society of America]. The Death Valley Publishing Company, Shoshone, CA, 27–35.

Figure captions

Figure 1: A: Location of Death Valley in the Basin and Range province, with location of the six study areas referred to in this paper indicated. B: Palaeogeographic reconstructions of the eastern Death Valley area during deposition of the Kingston Peak Formation, based upon integration of data from the Kingston Range, Sperry Wash and Silurian Hills areas. Modified from Le Heron & Busfield (2016).

Figure 2: Sedimentary logs of the Kingston Peak Formation from four separate ranges in the eastern Death Valley region. A: Sperry Wash, modified and simplified after Busfield & Le Heron (2016). B: Saddle Peak Hills, reproduced at high resolution- a previously unpublished partial section of a high quality, but intensely faulted, succession. C: Silurian Hills, modified from Le Heron et al. (2017). D: Southern Kingston Range- a previously unpublished section. Note that the scale bars on each of the logs: C and D are coarse resolution logs shown at the same scale as each other for direct comparison.

Figure 3: Representative sedimentary facies of the Sperry Wash area. A: General view showing well-bedded nature of the strata. Prominent ridges are composed of conglomerate. B: Channelised conglomerate, cutting down into ferruginous shales. C: Classic normally-graded bed of conglomerate, fining up to medium-grained sandstone. D: Large outsized clast of dolostone encased in mudstone deflecting underlying layers. E: Dm-thick diamictite encased in siltstone. F: Intensely deformed interval of laminites, interpreted as a glacitectonite (Busfield & Le Heron, 2016). G: Intricate ball and pillow structures. H:

Stratified diamictite interpreted as sub-ice shelf rainout deposits (Busfield & Le Heron, 2016).

Figure 4: Representative sedimentary facies in the Saddle Peak Hills range. A: Beck Spring Dolomite directly overlain by the Kingston Peak Formation. Strata are dipping northward (i.e. into the page) at about 25°. B: Ferruginous siltstones with thin graded sandstone beds sharply overlain by a thick, normally-graded conglomerate bed. Note hammer (30 cm long) for shale. C: Detail of diamictite, with abundant carbonate clasts derived from the underlying Beck Spring Dolomite. D: Classic normally-graded beds (more prominent horizons) punctuating more recessive, stratified siltstones. E: Lonestone of dolostone within stratified silty shale. F: Graded sandstone bed overlain by lonestone-bearing silty shale.

Figure 5: Kingston Peak facies in the Kingston Range area. A: Interbedded sandstones and siltstones which dominate much of the upper part of the formation above the olistostrome complex. B: Detail of a graded bed, interpreted as a turbidite (Le Heron et al., 2014): typical of the supra-olistostrome strata. C: Dropstone of Beck Spring Dolomite loading ferruginous shales. D: Rhythmically bedded siltstones and fine-grained sandstone, punctuated by small pebbles (dropstones). D: Diamictite toward the top of the Kingston Peak Formation, cropping out with typical low-lying exposure. F: Stratified diamictite with a quartzite dropstone toward the very top of the Kingston Peak Formation, about 10 m below the unconformity with the overlying Noonday Dolomite. G: Polished pebble in the diamictite. H: Possible striations on the surface of the striated pebble.

Figure 6: A: Typical outcrop of massive diamictite in the Alexander Hills. B: Detail of the massive diamictite (foliations are tectonic), with characteristically rounded pebbles of basement lithologies (gneiss, granitoid) and basement cover strata (dolostone, quartzite).

Figure 7: Kingston Peak facies in the Silurian Hills area. A: Steeply dipping strata comprising interstratified, boulder-bearing diamictite (to the left of the hammer) and heterolithic strata (turbidite sandstones and siltstones) to the right of the photo. B: Detail of typical boulder-bearing diamictite. Each of the visible clasts comprise schist and gneiss. C: Delicately laminated siltstones and sandstones. D: Quartzite cobble interpreted as a dropstone, with clear deflection and downwarping of siltstone layers.

Figure 8: Simple sketch log through part of the succession exposed in the Salt Spring Hills. To the authors' knowledge, no sedimentary log has previously been published for rocks in these hills, although Mrofka (2010) records the composition of the diamictites in this range, noting overall similarities to the Silurian Hills sections. Refer to Fig. 2 for the legend.

Figure 9: Kingston Peak facies in the southern Salt Spring Hills area. A: Typical outcrop style, characterised by frustratingly discontinuous layers, although high quality lithological observations can still be made. B: Structureless / massive diamictite dominated much of the exposed Kingston Peak succession. C: Exquisite dropstone textures in interstratified siltstone and fine-grained sandstone. D: Well stratified, ferruginous siltstones and shales with scattered lonestones toward the middle of the studied section.

Figure 10: Aspects of the Kingston Peak Formation in the Panamint Range. A: Thick accumulation of boulder-bearing diamictites in the Goler Wash area at the southern extremity of the range. B: Metabasite in the Pleasant Canyon section, in the central part of the range, crosscut by serpentinite veins, producing a ghostly "pillow-like" aspect to the exposure. These probably correspond to the MORB basic rocks reported by others (Labotka et al., 1980). C: The Wildrose diamictite in the northern part of the range (Wildrose Canyon)- note attenuated clasts, dominantly of a carbonate composition.

Figure 11: A and B: Satellite image and geological sketch map of part of the northern part of the Kingston Range exposures (modified from Le Heron et al., 2014), showing en echelon, NE-SW oriented normal fault arrays. Note the thickness changes of the various synglacial units across the faults, and the abrupt termination of some units against the footwall blocks. C: Geological facies map of the Silurian Hills, from Le Heron et al. (2017). Note the mappable megaclasts in this region, and the occurrence of two types of diamictite on the legend: a boulder-bearing diamictite (interpreted to represent glacial material) and a megaclast-bearing diamictite (interpreted to be repeated stratigraphic occurrences of olistostromes) (Le Heron et al., 2017). D and E: Google Earth image, looking south, with corresponding photo of a megaclast-bearing interval (megaclasts are arrowed). F: Sketch cross section through part of the Panamint Range (redrawn from Miller, 1985), showing syn-sedimentary extensional fault system that was active during deposition of the Kingston Peak Formation.

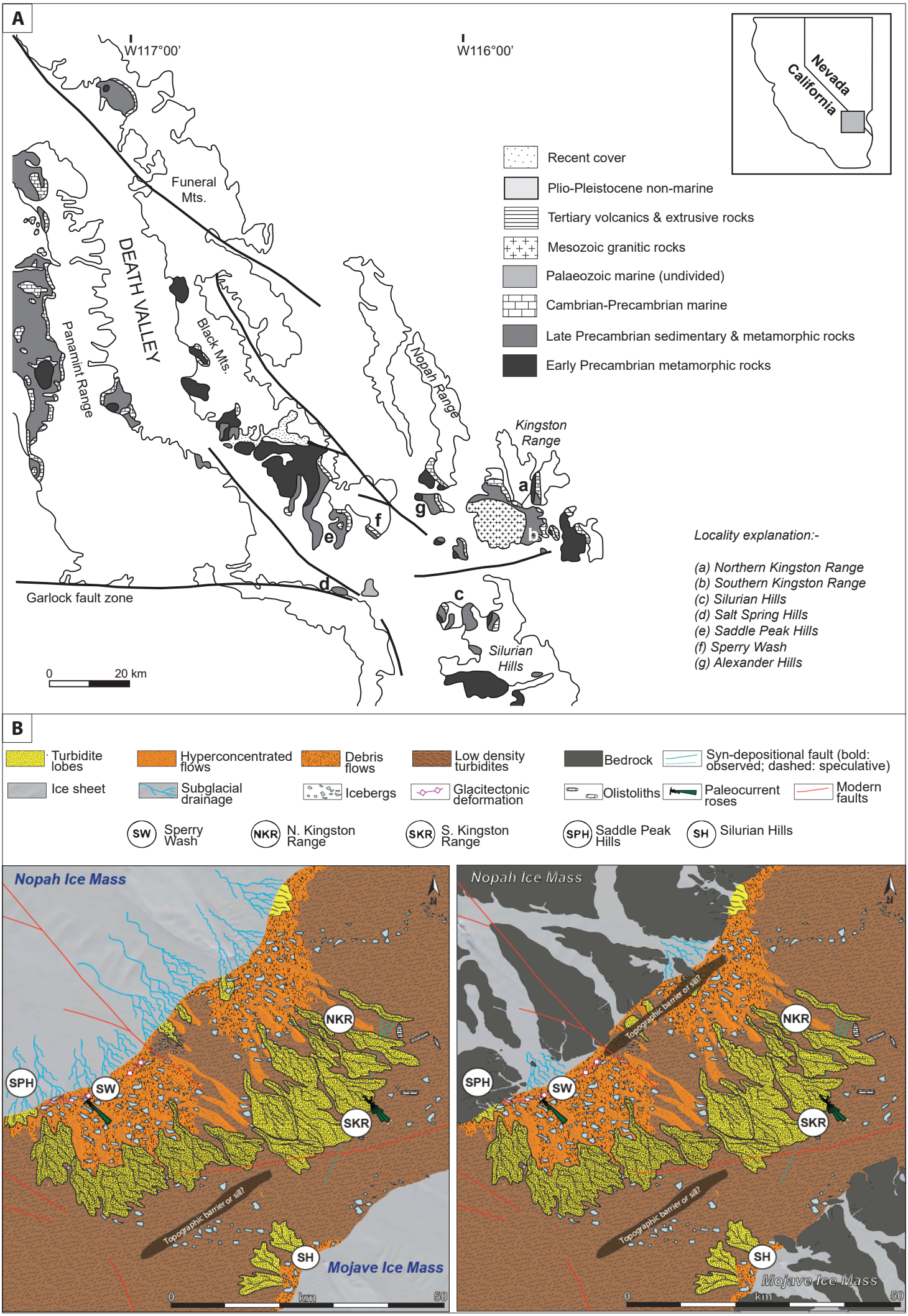
A
W117°00'
W116°00'
Nevada
California
Recent cover
Plio-Pleistocene non-marine
Tertiary volcanics & extrusive rocks
Mesozoic granitic rocks
Palaeozoic marine (undivided)
Cambrian-Precambrian marine
Late Precambrian sedimentary & metamorphic rocks
Early Precambrian metamorphic rocks
Funeral Mts.
DEATH VALLEY
Panamint Range
Black Mts.
Nopah Range
Kingston Range
Silurian Hills
Garlock fault zone
0
20 km
Locality explanation:-
(a) Northern Kingston Range
(b) Southern Kingston Range
(c) Silurian Hills
(d) Salt Spring Hills
(e) Saddle Peak Hills
(f) Sperry Wash
(g) Alexander Hills
B
Turbidite lobes
Hyperconcentrated flows
Debris flows
Low density turbidites
Bedrock
Syn-depositional fault (bold: observed; dashed: speculative)
Ice sheet
Subglacial drainage
Icebergs
Glacitectonic deformation
Olistoliths
Paleocurrent roses
Modern faults
SW Sperry Wash
NKR N. Kingston Range
SKR S. Kingston Range
SPH Saddle Peak Hills
SH Silurian Hills
Nopah Ice Mass
Topographic barrier or sill?
Mojave Ice Mass
0
km
50

Figure 1

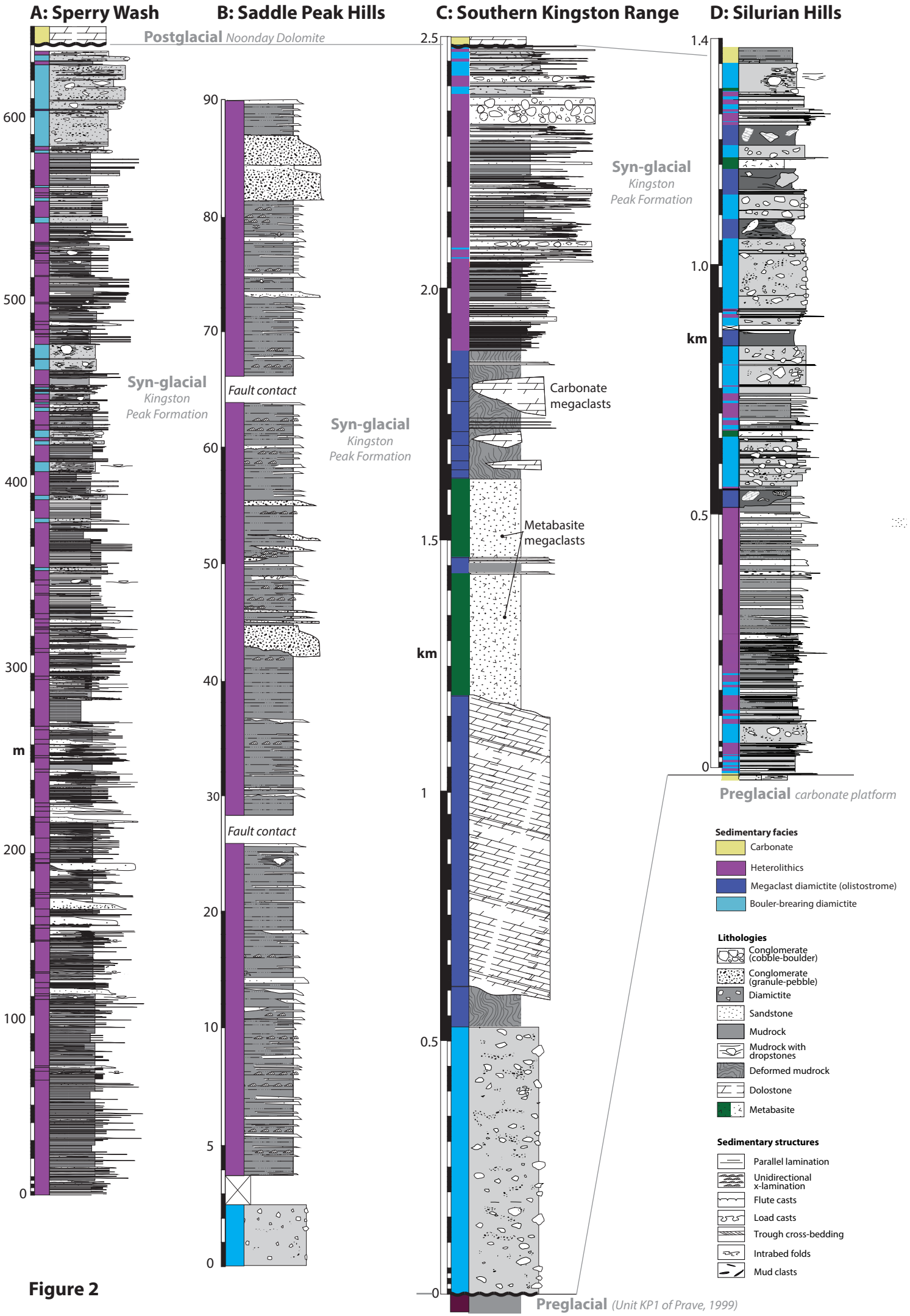
A: Sperry Wash
B: Saddle Peak Hills
C: Southern Kingston Range
D: Silurian Hills
Postglacial Noonday Dolomite
Syn-glacial
Kingston
Peak Formation
Fault contact
Fault contact
Syn-glacial
Kingston
Peak Formation
Carbonate
megaclasts
Metabasite
megaclasts
Syn-glacial
Kingston
Peak Formation
Preglacial carbonate platform
Preglacial (Unit KP1 of Prave, 1999)
m
km
km
Sedimentary facies
Carbonate
Heterolithics
Megaclast diamictite (olistostrome)
Bouler-brearing diamictite
Lithologies
Conglomerate (cobble-boulder)
Conglomerate (granule-pebble)
Diamictite
Sandstone
Mudrock
Mudrock with dropstones
Deformed mudrock
Dolostone
Metabasite
Sedimentary structures
Parallel lamination
Unidirectional x-lamination
Flute casts
Load casts
Trough cross-bedding
Intrabed folds
Mud clasts

Figure 2

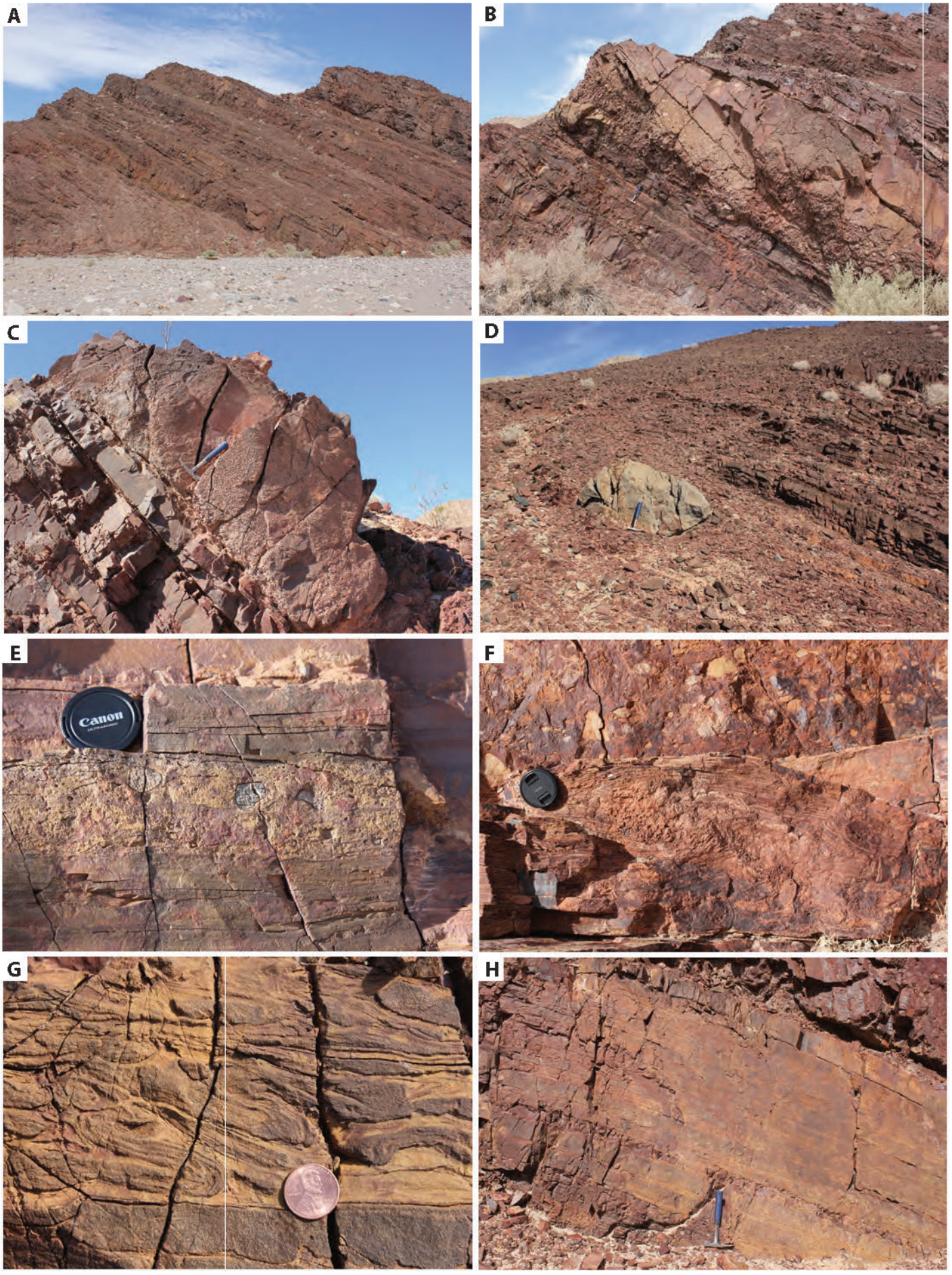

Figure 3

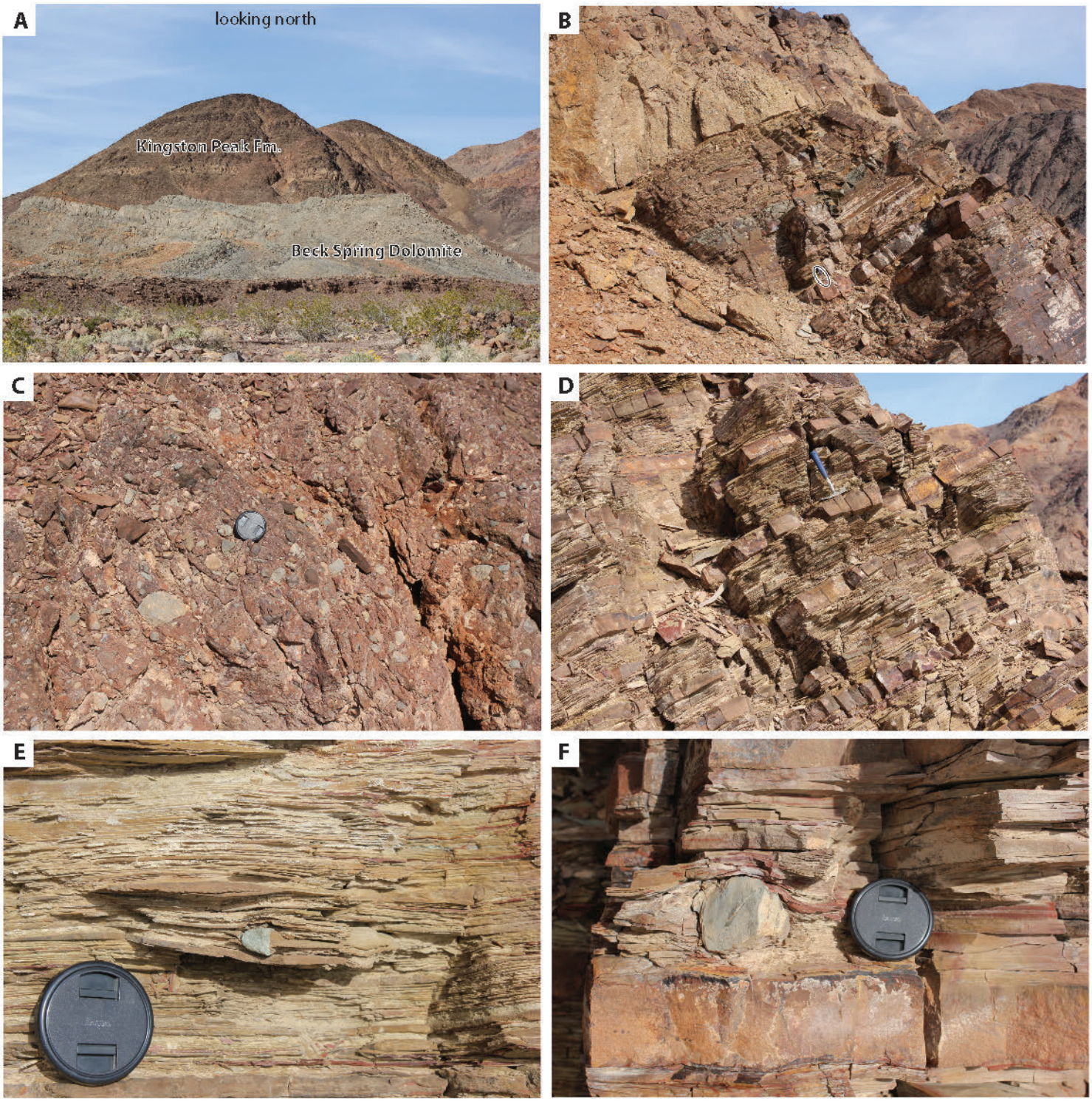
A
looking north
Kingston Peak Fm.
Beck Spring Dolomite
B
C
D
E
F

Figure 4

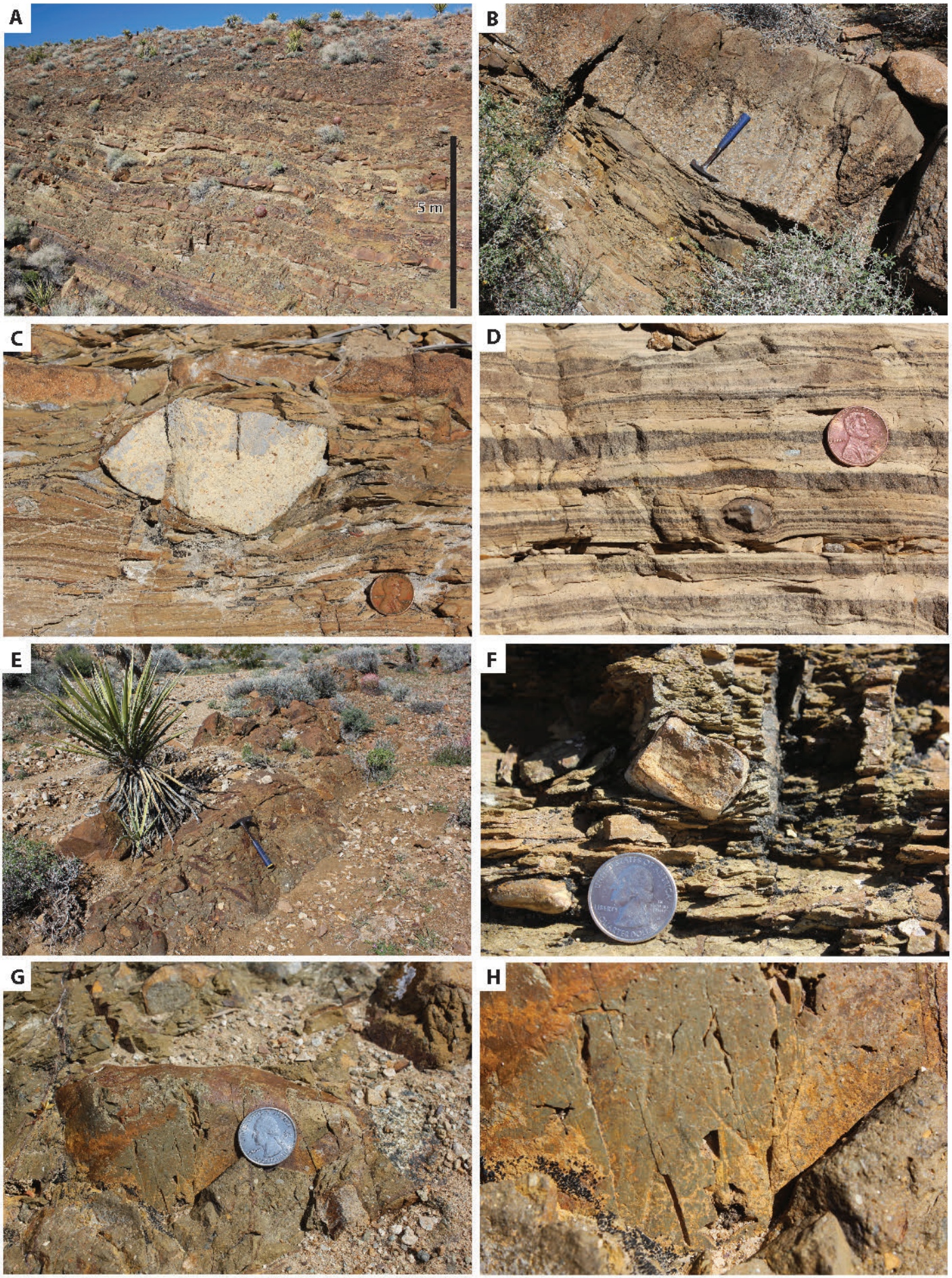

Figure 5

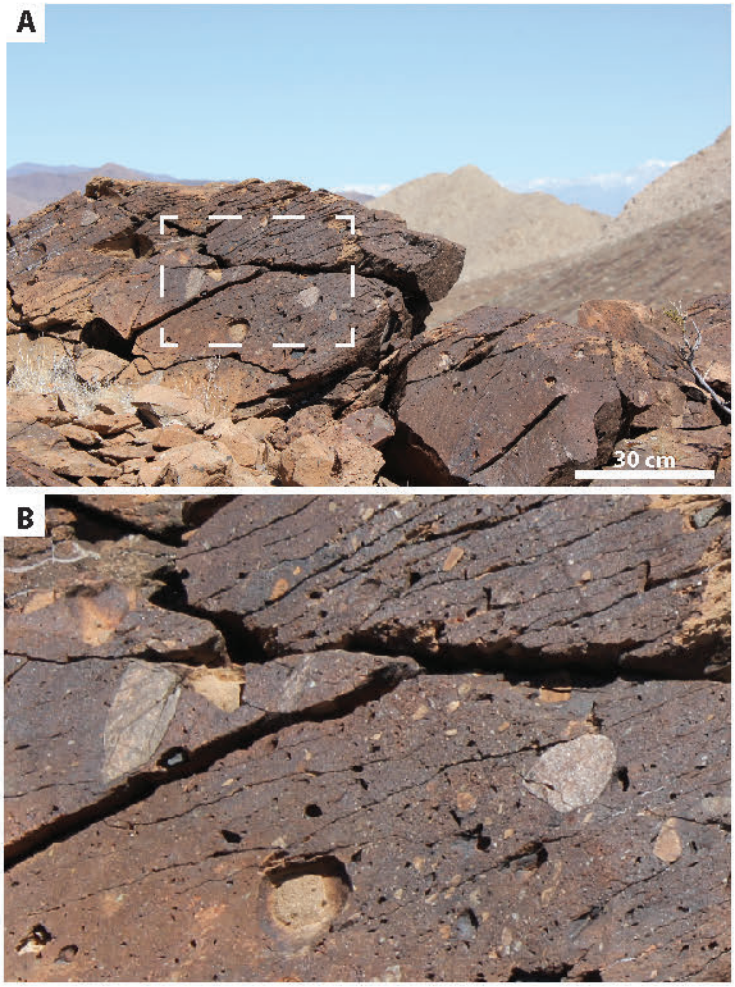

Figure 6

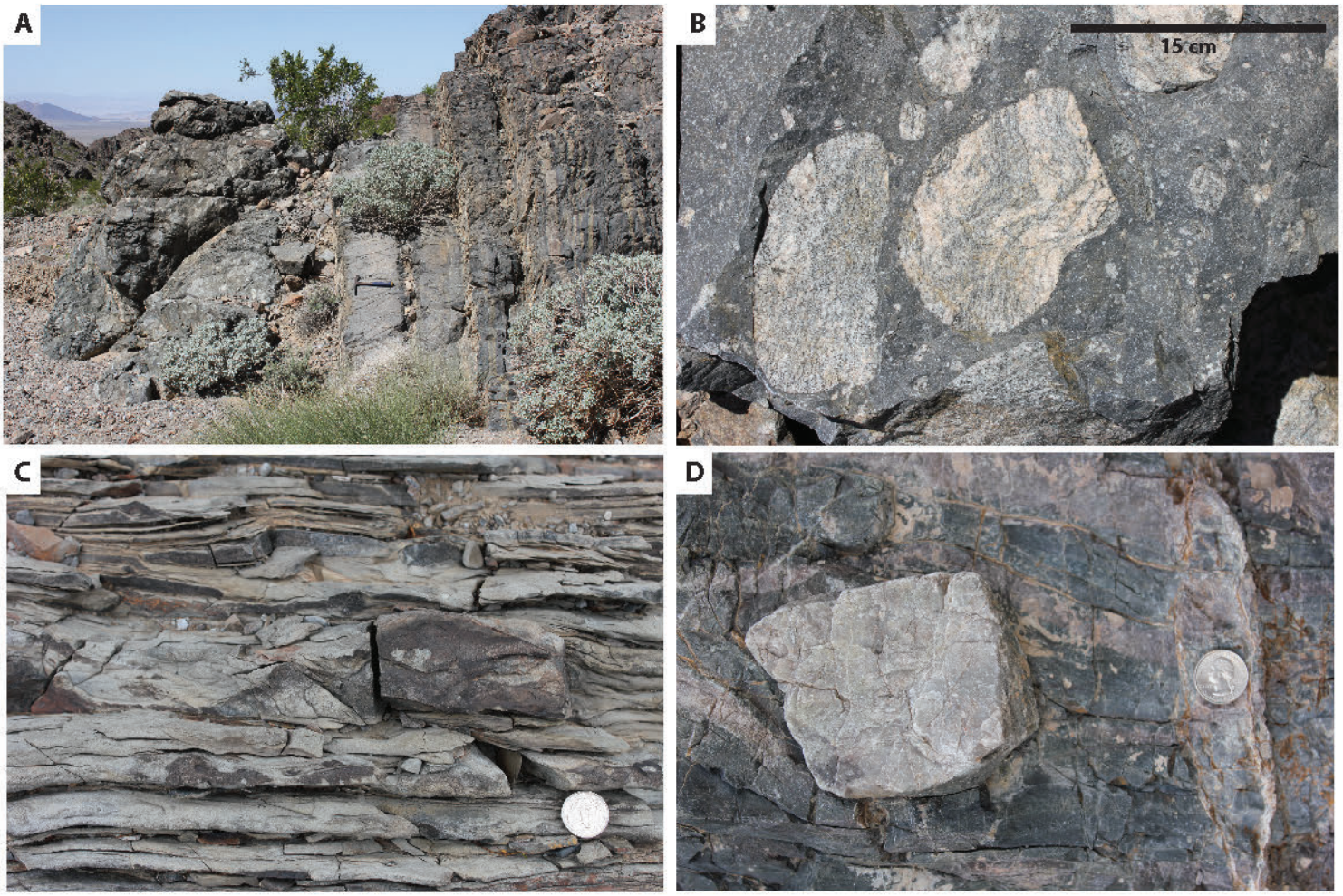

Figure 7

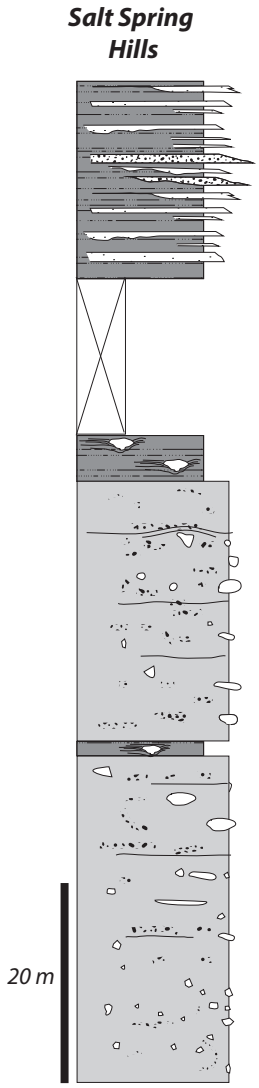

Figure 8

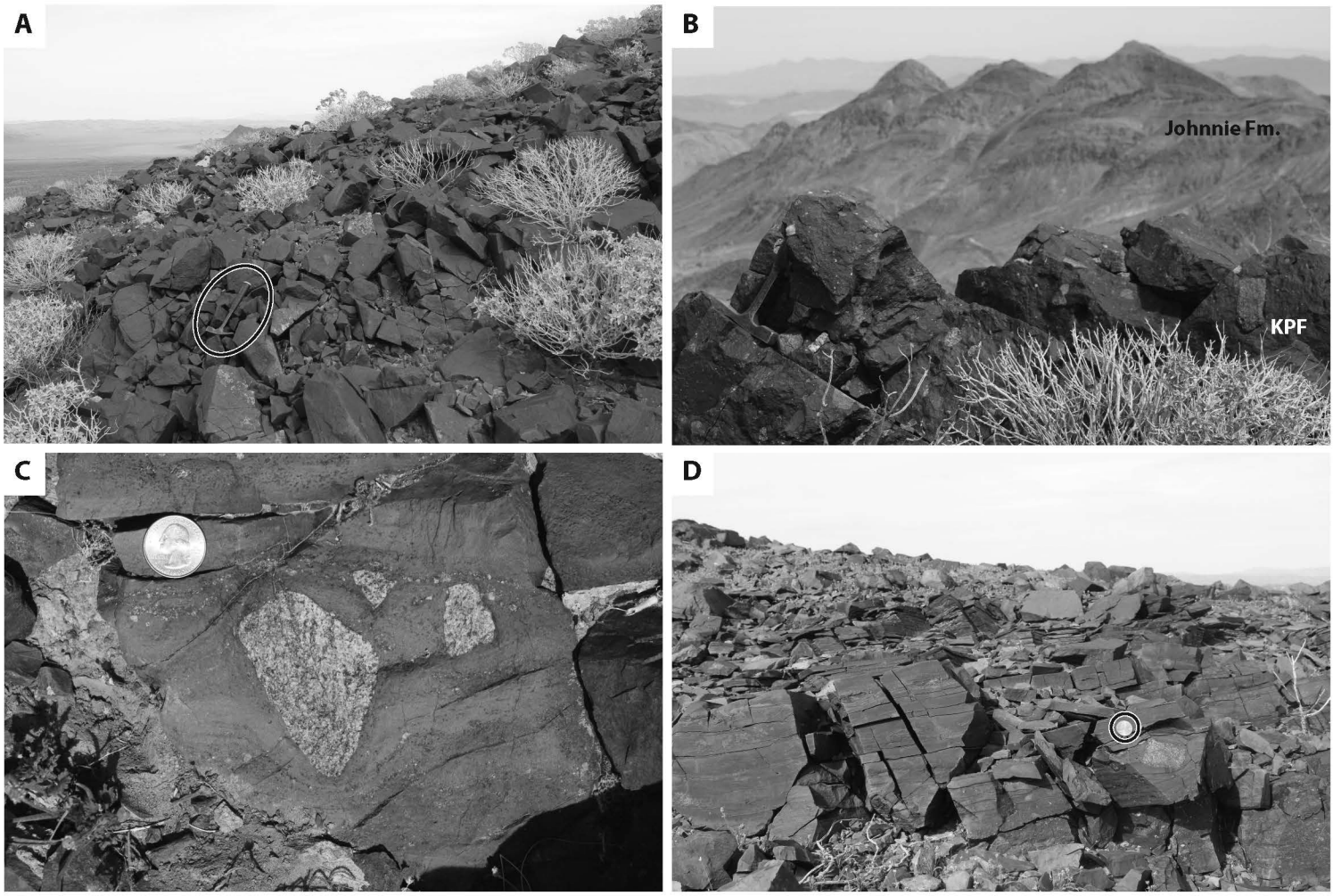

Figure 9

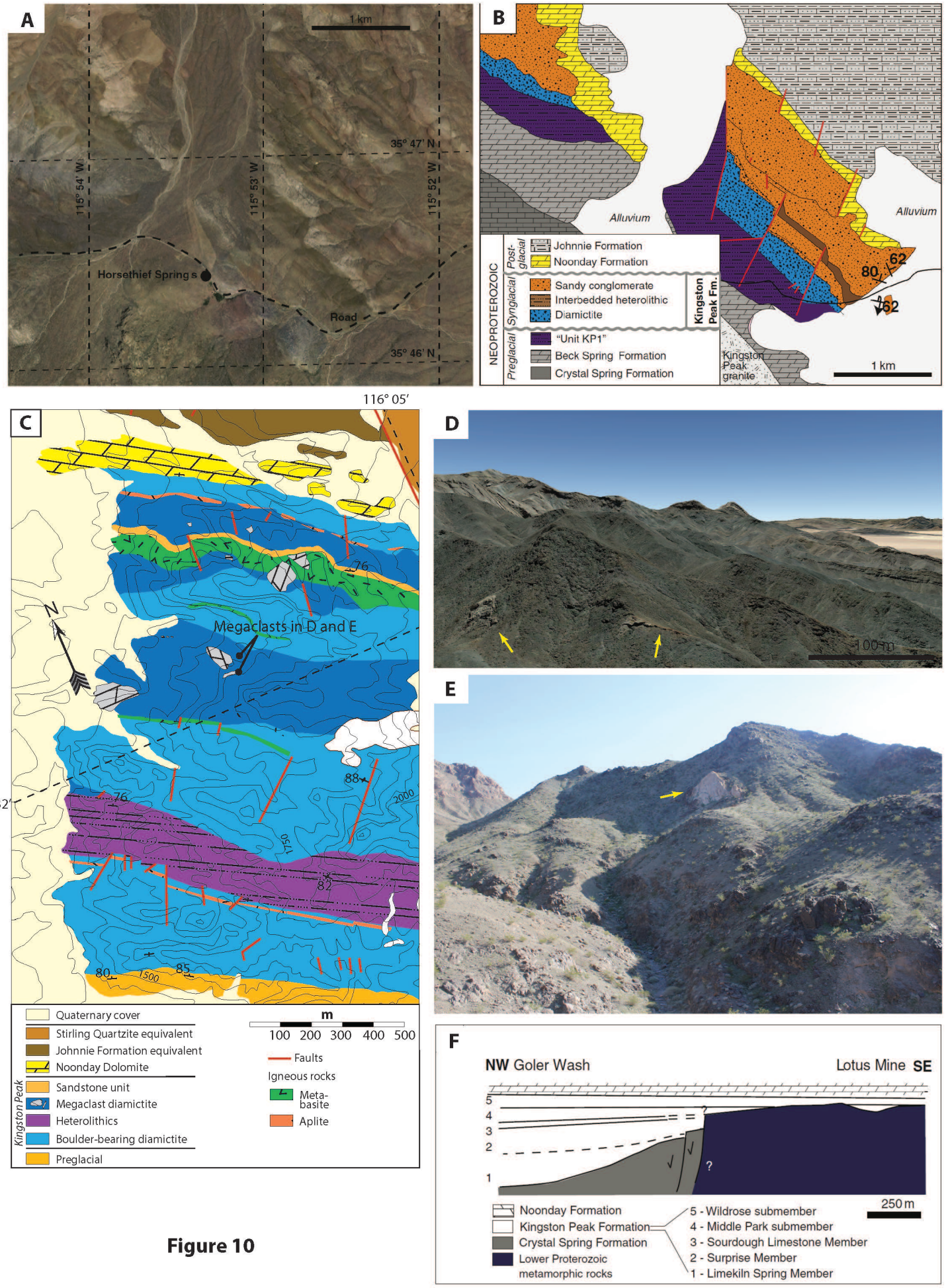
A
1 km
35° 47' N
115° 54' W
115° 53' W
115° 52' W
Horsethief Springs
Road
35° 46' N
B
Alluvium
Alluvium
NEOPROTEROZOIC
Post-glacial
Johnnie Formation
Noonday Formation
Synglacial
Sandy conglomerate
Interbedded heterolithic
Diamictite
Kingston Peak Fm.
Preglacial
"Unit KP1"
Beck Spring Formation
Crystal Spring Formation
Kingston Peak granite
62
80
62
1 km
116° 05'
C
35° 32'
N
Megaclasts in D and E
76
76
88
2000
1750
82
80
1500
85
Quaternary cover
Stirling Quartzite equivalent
Johnnie Formation equivalent
Noonday Dolomite
Kingston Peak
Sandstone unit
Megaclast diamictite
Heterolithics
Boulder-bearing diamictite
Preglacial
m
100 200 300 400 500
Faults
Igneous rocks
Meta-basite
Aplite
D
100 m
E
F
NW Goler Wash
Lotus Mine SE
5
4
3
2
1
?
?
250 m
Noonday Formation
Kingston Peak Formation
Crystal Spring Formation
Lower Proterozoic metamorphic rocks
5 - Wildrose submember
4 - Middle Park submember
3 - Sourdough Limestone Member
2 - Surprise Member
1 - Limekiln Spring Member

Figure 10